

# Gecko-Inspired Carbon Nanotube-Based Self-Cleaning Adhesives

Sunny Sethi,<sup>†</sup> Liehui Ge,<sup>†</sup> Lijie Ci,<sup>‡</sup> P. M. Ajayan,<sup>‡</sup> and Ali Dhinojwala<sup>\*,†</sup>

Department of Polymer Science, The University of Akron, Akron, Ohio 44325,

Department of Materials Science and Engineering, Rensselaer Polytechnic Institute, Troy, New York 12180-3590

Received October 26, 2007

## ABSTRACT

The design of reversible adhesives requires both stickiness and the ability to remain clean from dust and other contaminants. Inspired by gecko feet, we demonstrate the self-cleaning ability of carbon nanotube-based flexible gecko tapes.

A gecko has the unique ability to reversibly stick and unstick to a variety of smooth and rough surfaces. The gecko's wall climbing ability, without the use of viscoelastic glue, has attracted significant attention.<sup>1–11</sup> Although the gecko does not groom its feet, its stickiness remains for months between molts.<sup>12</sup> The gecko's dirty feet can recover its ability to climb vertical walls only after a few steps.<sup>12</sup> Our daily experience with sticky tapes has been the opposite. The stickier the adhesive, the more difficult it is to keep it clean from dust and other contaminants. Synthetic self-cleaning adhesives, inspired by the gecko's feet, could be used for many applications including wall climbing robots and microelectronics.

The secret of the gecko's adhesive properties lies in the microstructure of gecko feet.<sup>1,13–15</sup> Microscopy shows that gecko feet are covered with millions of small hairs called setae, which further divide into hundreds of smaller spatulas (Figure 1A). When such a structure is placed against any surface, hairs adapt and allow a very large area of contact with the surface. The van der Waals (vdW) interaction between the hairs and the substrate after contact is sufficient for the gecko to adhere. It has been suggested that this same hairy carpet on the gecko feet also plays an important role in self-cleaning.<sup>12</sup>

Some of the other systems found in nature that exhibit self-cleaning properties are the leaves of lotus and lady's mantle plants.<sup>18</sup> The surface of lotus leaves have two levels of microscopic roughness (Figure 1B). This hierarchical roughness along with a hydrophobic wax coating makes the lotus leaves superhydrophobic.<sup>16,19–21</sup> A water droplet forms a large contact angle with low contact angle hysteresis. This

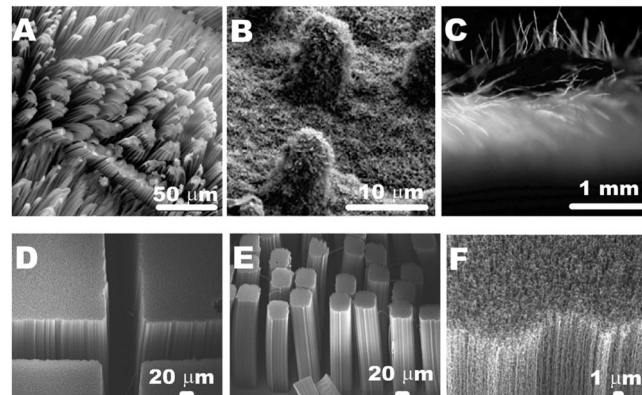


**Figure 1.** Natural and synthetic structures showing self-cleaning abilities. (A) SEM image of natural gecko setae. (B) Surface of a lotus leaf with hierarchical roughness.<sup>16</sup> (C) Hairy structure of lady's mantle leaf.<sup>17</sup> (D–E) SEM images of synthetic setae made of micropatterned carbon nanotube bundles of varying size. (F) Higher magnification SEM image of synthetic setae showing thousands of vertically aligned carbon nanotubes that act as spatulas.

results in the water droplets rolling off the surface, leaving the surface clean. Leaves of a lady's mantle plant have hairs of 10  $\mu\text{m}$  diameter and length of 1 mm (Figure 1C). It has been suggested that the individual hairs are hydrophilic. However, when acting together on the surface, they make the surface of the leaves superhydrophobic.<sup>17</sup> Even though the surface properties of the spatulas are not known, the hierarchical structure of gecko feet makes the macroscopic structure superhydrophobic.<sup>12</sup>

Significant effort in developing synthetic materials inspired by gecko feet show comparable, and in some cases better, shear resistance than natural gecko feet.<sup>2,6–9,11</sup> Still, these measurements were done in controlled environments and limited self-cleaning data of these synthetic materials were reported.<sup>7</sup> Recently, we have designed carbon nanotube-based

\* Corresponding author. E-mail: ali4@uakron.edu.

<sup>†</sup> Department of Polymer Science, The University of Akron.

<sup>‡</sup> Department of Materials Science and Engineering, Rensselaer Polytechnic Institute.

synthetic tapes that support four times more shear stress than the gecko.<sup>11</sup> To obtain these high shear forces, it is important to mimic the hierarchical structure of setae and spatulae on the gecko feet. The length and diameter of carbon nanotubes, size of the pattern, and stiffness of the backing tape are all important parameters that need to be optimized for superior performance. Parts D–F of Figure 1 show carbon nanotube patterns of 500 and 50  $\mu\text{m}$  in size consisting of even smaller (8–10 nm) carbon nanotube hairs within those patterns.<sup>11</sup> In this paper, we show that, for optimum length and pattern size, these carbon nanotube-based synthetic tapes exhibit self-cleaning as well as high shear resistance. These tapes can be cleaned by water, as shown by the leaves of lotus and lady's mantle plants. In addition, the synthetic tapes can also be cleaned by a contact mechanism similar to that exhibited by the gecko. After mechanical cleaning, the shear strength recovers back to 90% (and 60% for water-cleaned samples) of the values measured before soiling. In comparison, the gecko recovers back 50% of the shear stress after eight steps.<sup>12</sup> The ability of these synthetic tapes to self-clean and also retain their shear resistance makes it an excellent choice for gecko-inspired adhesives.

Micropatterned vertically aligned carbon nanotubes are grown on a silicon substrate with  $\text{SiO}_2$ . Photolithography is used to deposit catalyst in square patterns of 50–500  $\mu\text{m}$  edge on a  $\text{SiO}$  wafer. The catalyst layer consists of a 10 nm thick aluminum (Al), which acts as a buffer layer, and 1.5 nm thick iron catalyst layer, which forms nanosize particles for catalytic growth of carbon nanotubes. Ethylene (flow rate of 50–150 standard cc min) is used as a carbon source, and the reaction is carried out at 750 °C. An  $\text{Ar}/\text{H}_2$  gas mixture (15%  $\text{H}_2$ ) with a flow rate of 1300 standard cc per min is used as the buffer gas. Water vapor with a dew point of –20 °C is introduced in the reaction furnace by  $\text{Ar}/\text{H}_2$  flow during carbon nanotube growth. The growth time is 3 min, and the length of the carbon nanotubes is 100  $\mu\text{m}$ . The average diameter of the carbon nanotubes is 8 nm (2–5 walls). Flexible polymer tape with tacky coating on one side is pressed against the top surface of the carbon nanotubes. Upon peeling, the carbon nanotubes are transferred from the silicon substrate to the flexible polymer tape. Parts D–F of Figure 1 show SEM images of carbon nanotubes of 500 and 50  $\mu\text{m}$  patterns. A higher magnification SEM image is shown in Figure 1F. In this paper, we report the results for only 250  $\mu\text{m}$  patches with 100  $\mu\text{m}$  in height. These samples have the optimum dimensions needed for both adhesion and self-cleaning.

A 10  $\mu\text{L}$  water droplet on a 250  $\mu\text{m}$  pattern is shown in Figure 2A. The static contact angle of  $155 \pm 3^\circ$  is observed, indicating the superhydrophobic properties of these hierarchical structures of carbon nanotubes. We also observed similar contact angles even after exposing the samples with water after multiple use. It has been shown that the vertically aligned carbon nanotubes coated with hydrophobic fluorinated polymers<sup>22,23</sup> or nonaligned carbon nanotubes<sup>24</sup> show high water contact angles. However, coating the carbon nanotubes with fluorinated polymers or nonaligned carbon nanotubes is not desirable for making sticky tapes. In

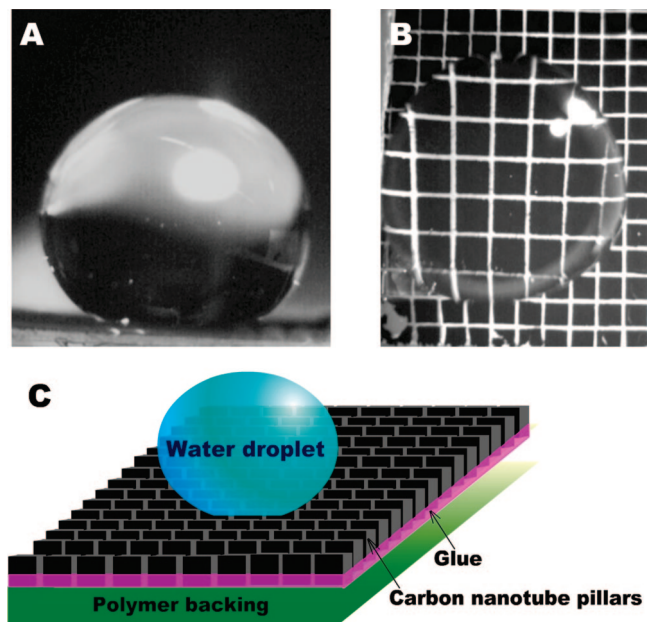


**Figure 2.** Superhydrophobic behavior of micropatterned carbon nanotube pillars of 250  $\mu\text{m}$  in width and 100  $\mu\text{m}$  in height. (A) A 10  $\mu\text{L}$  water droplet sitting on the surface of vertically aligned carbon nanotubes. (B) Top view of water droplet sitting on the micropatterned carbon nanotube pillars. (C) Schematic diagram showing carbon nanotube pillars held at base by polymer adhesive and a water droplet sitting on top of pillars.

addition, the uncoated vertically aligned carbon nanotubes on silicon wafers collapse under the influence of capillary forces.<sup>22,25–27</sup> In these experiments, the carbon nanotubes pillars are held by a polymeric glue at the base and this does not allow individual structures to collapse due to capillary forces (Figure 2C). This process eliminated the use of fluorinated coatings (or other nonwetting materials) on the carbon nanotubes to make these structures superhydrophobic.

To demonstrate the self-cleaning ability of the synthetic tapes, we soiled these tapes (Figure 3A) with silica particles ranging from 1 to 100  $\mu\text{m}$  in size (shown in Figure 3B). The silica particles are used in these experiments to represent dust. When rinsed with water, the water droplets roll off very easily, carrying with them most of the silica particles. The picture of the clean surface after rinsing with water is shown in Figure 3C. We have observed no macroscopic damage of the carbon nanotube pillars after rinsing with water. However, we occasionally observe small microcracks within the pillars that are formed due to drying of water (shown as an inset in Figure 3C). We have also tested the self-cleaning properties of these synthetic tapes by contact mechanics, similar to the procedure used by Autumn to understand the self-cleaning process of a gecko's feet. After a couple of contacts with mica (or glass substrate), we observe that the majority of these particles are transferred to the mica (or the glass) surface. This effect is even easier to observe by applying a small vibration. Most of the silica particles fall off of the surface with only few small-size silica particles still sticking to the surface and in between the pillars of the carbon nanotube. The synthetic tapes before and after mechanical cleaning are shown in parts A and D of Figure 3.

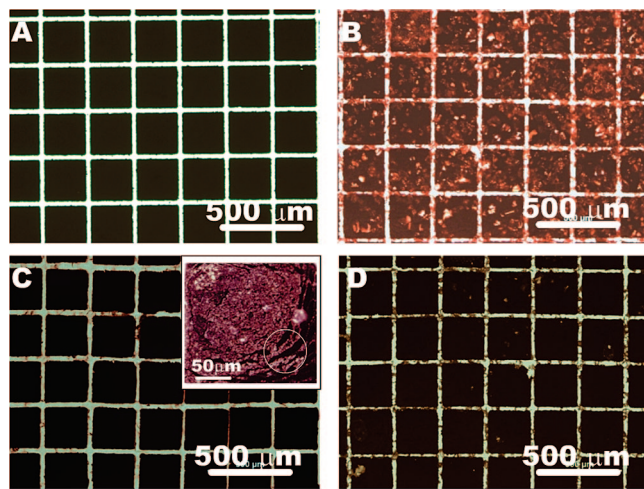


**Figure 3.** Optical images showing dusted samples after different treatments. (A) Image of pristine  $250\ \mu\text{m}$  sample. (B) Image of dusted  $250\ \mu\text{m}$  sample. (C) Image of dusted sample cleaned with water. The inset shows a higher magnification image of the carbon nanotube pillar and the example of microcracks that are developed during drying are seen inside the region marked by a white circle. (D) Image of dusted sample cleaned by applying vibrations.

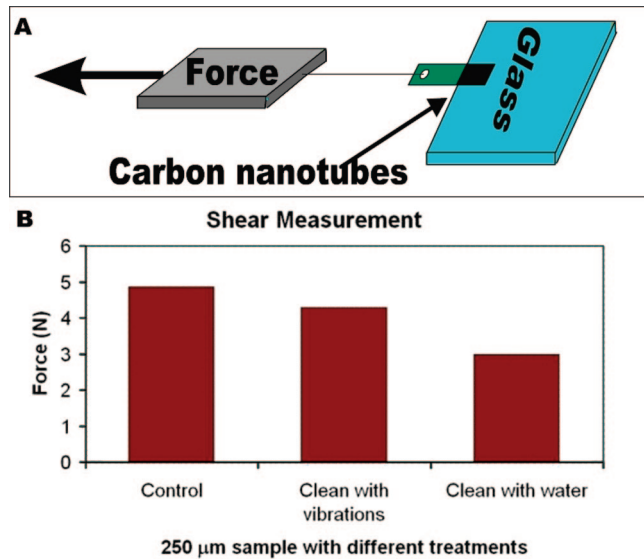


**Figure 4.** Shear measurement apparatus and data. (A) Sketch of apparatus used to measure shear data, the scale is mounted on a movable platform. Carbon nanotube sample is attached to the scale and the scale is moved back with constant velocity. Computer program measures the maximum load before breakdown. (B) Data for shear measurements for control, sample dusted and cleaned by applying vibrations or with water.

Although the synthetic tapes appear to be free of silica particles after cleaning with water or contact mechanics, it is important to demonstrate whether these tapes regain the same shear resistance as the pristine samples before soiling with silica particles. The results show that the shear stress of the cleaned samples are 60–90% of those for the pristine, unsoiled samples. We demonstrate this by measuring the shear forces using a home-built shear device shown in Figure 4A. The carbon nanotube tapes ( $0.16\ \text{cm}^2$  in area) are pressed against a clean mica surface with a preload of  $25\text{--}50\ \text{N/cm}^2$ . The tapes are then pulled with a velocity of  $400\ \mu\text{m/s}$ . Figure

4B shows the shear forces for the pristine sample, the sample soiled by silica particles and subsequently cleaned by water, and the sample soiled by silica particles and cleaned by mechanical vibration. The shear stress for the pristine sample was around  $5\ \text{N}$ . When the tape was dusted and cleaned using vibrations, it regained 90% of the shear stress. The slightly lower shear forces are due to smaller silica particles remaining stuck on the surface and in the spacing between the carbon nanotube patches. This recovery of shear resistance in the synthetic tapes is very promising because the live gecko only shows a recovery of 50% of the shear stress after eight steps.<sup>12</sup> When the tape was dusted and cleaned by water it regained 60% of the shear stress. The lower efficiency of the water cleaned samples are perhaps due to formation of microcracks within the patches during drying of water (inset in Figure 3C). It is possible to reduce the spacing between the carbon nanotube patches so that it does not provide the space for smaller silica particles to penetrate between the pillars. In addition, the binding glue that holds the carbon nanotube pillars at the base to reduce the microcracks developed during the drying process can be optimized.

In summary, the synthetic micropatterned carbon nanotube-based gecko tapes show not only higher shear resistance than the natural gecko feet but also mimic the remarkable self-cleaning abilities of the gecko, lotus, and lady's mantle leaves.

**Acknowledgment.** We gratefully thank the financial support from NSF (DMR-9984996 and Nanoscale Interdisciplinary Research Teams grant 0609077).

## References

- Autumn, K.; Liang, Y. A.; Hsieh, T. S.; Zesch, W.; Chan, W. P.; Kenny, T. W.; Fearing, R.; Full, R. J. *Nature* **2000**, *405*, 681–685.
- del Campo, A.; Greiner, C.; Alvarez, I.; Arzt, E. *Adv. Mater.* **2007**, *19*, 1973–1977.
- Arzt, E. *Mater. Sci. Eng., C* **2006**, *26*, 1245–1250.
- Geim, A. K.; Dubonos, S. V.; Grigorieva, I. V.; Novoselov, K. S.; Zhukov, A. A.; Shapoval, S. Y. *Nat. Mater.* **2003**, *461*–463.
- Sitti, M.; Fearing, R. S. *J. Adhes. Sci. Technol.* **2003**, *17*, 1055–1073.
- Yurdumakan, B.; Raravikar, N. R.; Ajayan, P. M.; Dhinojwala, A. *Chem. Commun.* **2005**, 3799–3801.
- Gorb, S.; Varenberg, M.; Peressadko, A.; Tuma, J. *J. R. Soc. Interface* **2007**, *4*, 271–275.
- Lee, H.; Lee, B. P.; Messersmith, P. B. *Nature* **2007**, *448*, 338–341.
- Northen, M. T.; Turner, K. L. *Nanotechnology* **2005**, *16*, 1159–1166.
- Northen, M. T.; Turner, K. L. *Sens. Actuators, A* **2006**, *A130*–*A131*, 583–587.
- Ge, L.; Sethi, S.; Ci, L.; Ajayan, P. M.; Dhinojwala, A. *Proc. Natl. Acad. Sci. U.S.A.* **2007**, *104*, 10792–10795.
- Hansen, W. R.; Autumn, K. *Proc. Natl. Acad. Sci. U.S.A.* **2005**, *102*, 385–389.
- Gorb, S.; Jiao, Y.; Scherge, M. *J. Comp. Physiol., A* **2000**, *186*, 821–831.
- Autumn, K.; Sitti, M.; Liang, Y. A.; Peattie, A. M.; Hansen, W. R.; Sponberg, S.; Kenny, T. W.; Fearing, R.; Israelachvili, J. N.; Full, R. J. *Proc. Natl. Acad. Sci. U.S.A.* **2002**, *12252*–*12256*.
- Tian, Y.; Pesika, N.; Zeng, H.; Rosenberg, K.; Zhao, B.; McGuigan, P.; Autumn, K.; Israelachvili, J. *Proc. Natl. Acad. Sci. U.S.A.* **2006**, *103*, 19320–19325.
- Patankar, N. A. *Langmuir* **2004**, *20*, 7097–7102.
- Mock, U.; Foerster, R.; Menz, W.; Ruehe, J. *J. Phys.: Condens. Matter* **2005**, *17*, S639–S648.
- Alexander, O.; Stephan, H. *Langmuir* **2004**, *20*, 2405–2408.
- Marmur, A. *Langmuir* **2004**, *20*, 3517–3519.
- Cheng, Y.-T.; Rodak, D. E. *Appl. Phys. Lett.* **2005**, *86*, 144101/1–144101/3.

(21) Gao, L.; McCarthy, T. J. *J. Am. Chem. Soc.* **2006**, *128*, 9052–9053.

(22) Zhu, L.; Xiu, Y.; Xu, J.; Tamirisa, P. A.; Hess, D. W.; Wong, C.-P. *Langmuir* **2005**, *21*, 11208–11212.

(23) Lau, K. K. S.; Bico, J.; Teo, K. B. K.; Chhowalla, M.; Amarasinghe, G. A. J.; Milne, W. I.; McKinley, G. H.; Gleason, K. K. *Nano Lett.* **2003**, *3*, 1701–1705.

(24) Zhu, Y.; Zhang, J. C.; Zhai, J.; Zheng, Y. M.; Feng, L.; Jiang, L. *ChemPhysChem* **2006**, *7*, 336–341.

(25) Taolei, S.; Guojie, W.; Huan, L.; Lin, F.; Lei, J.; Daoben, Z. *J. Am. Chem. Soc.* **2003**, *125*, 14996–14997.

(26) Huang, L.; Lau, S. P.; Yang, H. Y.; Leong, E. S. P.; Yu, S. F.; Prawer, S. *J. Phys. Chem. B* **2005**, *109*, 7746–7748.

(27) Journet, C.; Moulinet, S.; Ybert, C.; Purcell, S. T.; Bocquet, L. *Europ. Lett.* **2005**, *71*, 104–109.

NL0727765